

# Enhanced drug loading in polymerized micellar cargo†

Julien Ogier,<sup>a</sup> Thomas Arnault,<sup>\*b</sup> Géraldine Carrot,<sup>c</sup> Antoine Lhumeau,<sup>b</sup> Jean-Marie Delbos,<sup>b</sup> Claire Boursier,<sup>b</sup> Olivier Loreau,<sup>a</sup> Francois Lefoulon<sup>b</sup> and Eric Doris<sup>\*a</sup>

Received 15th March 2010, Accepted 10th June 2010

First published as an Advance Article on the web 9th July 2010

DOI: 10.1039/c004134c

A new drug carrier system based on self-assembly and polymerization of polydiacetylenic amphiphiles is described. Although classical amphiphiles can help in solubilizing hydrophobic molecules upon self-assembly into a variety of nanometric structures, a greater effect on drug loading was observed for our polymerized micelles as compared to the non-polymerized analogues. This permitted higher aqueous solubilization of lipophilic drugs with low micelle concentration. <sup>14</sup>C labeling of a model drug on one side and of the amphiphile on the other side permitted assessment, after intravenous injection, of biodistribution and excretion profiles of the drug cargo.

## Introduction

The past two decades have witnessed significant progress in the development of new drug delivery systems to carry active molecules through different biological barriers and reach specific targets.<sup>1</sup> Substantial efforts have been devoted to overcome drawbacks associated with the intrinsic properties of therapeutic molecules, such as solubility (toxicity and absorption issues), stability (*in vivo* degradation), pharmacokinetics (rapid elimination) and/or biodistribution (non-specific distribution).<sup>2</sup> Particularly, most of the anticancer drugs exhibit low solubility in water due to their inherent hydrophobic properties that, on the other hand, enhance their cell internalization and efficacy.<sup>3</sup>

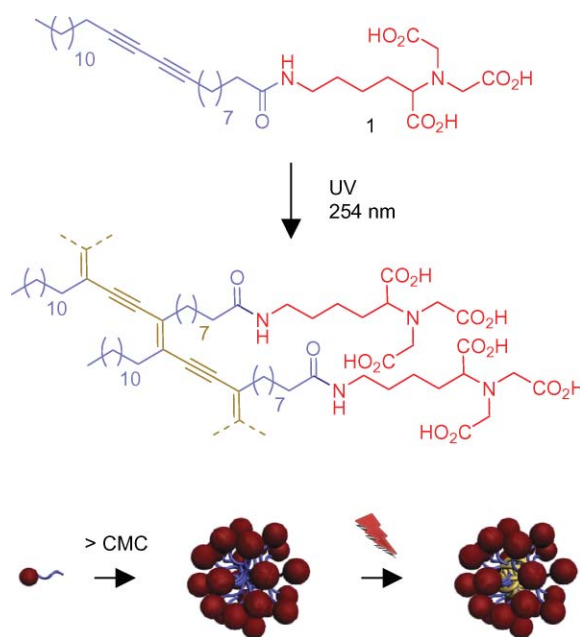
Two main strategies have been developed to increase the aqueous solubility of such compounds. The first approach consists in modifying the chemical structure of the drug by attaching hydrophilic functional groups or hydro-soluble molecules, *i.e.* targeting or cell-penetrating peptides,<sup>4</sup> polyethylene glycols<sup>5</sup> or other hydrophilic ligands.<sup>6</sup> However, the increase of the drug solubility could disrupt therapeutic activity, and a balance between solubility and activity has to be found.<sup>7,8</sup> The second approach is based on the solubilization of the active molecules using drug-cargo systems<sup>9</sup> such as nanoparticles,<sup>10</sup> micelles of block copolymers,<sup>11</sup> liposomes<sup>12</sup> or dendrimers.<sup>13</sup> This strategy successfully increases the molecules' stability and solubility, since their activity is unaffected, their bio-availability improved by a sustained release in time, and their toxicity lowered. Nevertheless, the carrier has to be highly soluble in water with a significant drug loading capacity.

In the present paper, we report a new cargo system based on polymerized micelles which exhibit high solubility and drug loading. Our approach is based on the self-assembly into micelles

of specifically designed monomer surfactants and subsequent polymerization.

## Results and discussion

The micellar nano-structures were obtained by dispersion of amphiphilic monomers at concentrations greater than the critical micellar concentration (CMC). To stabilize the supramolecular assembly, a photo-polymerizable amphiphile **1** was used.<sup>14</sup> It incorporates a photo-responsive diacetylenic group within the C25-hydrocarbon chain and a hydrophilic nitrilotriacetic acid (NTA) polar head (Scheme 1). The pH value of the solution has a key effect on the final structure of the self-assembly. At lower pH (below 10), amphiphiles self-assemble as ribbons which, upon heating to 70 °C, coil-up into tubular nanostructures<sup>15</sup> (see ESI†). At higher pH values (*e.g.* pH = 12), well defined micelles were obtained. To polymerize and uphold the micelle structure, the



Scheme 1 Polymerization of diacetylenic amphiphile.

<sup>a</sup>CEA, iBiTecS, Service de Chimie Bioorganique et de Marquage, 91191 Gif-sur-Yvette, France. E-mail: eric.doris@cea.fr

<sup>b</sup>Technologie Servier, 27 rue Eugène Vignat, 45000 Orléans, France. E-mail: thomas.arnault@fr.netgrs.com

<sup>c</sup>CEA, Laboratoire Léon Brillouin, 91191 Gif-sur-Yvette, France

† Electronic supplementary information (ESI) available: Experimental procedures, TEM pictures, <sup>1</sup>H NMR drug loading data. See DOI: 10.1039/c004134c

solution was irradiated at 254 nm for 5 h. The polymerization takes place by a topochemical 1,4-addition mechanism.<sup>16–20</sup>

In the course of the polymerization step, the micelle solution changed from colorless to yellowish. This indicates an increase in length of the conjugated polymer backbone (Fig. 1a,b). Kinetic studies of the micelle polymerization showed fast polymerization of the monomer in the initial five hours with up to 75% conversion. Beyond this point, the polymerization rate decreased and reached 90% conversion after 15 h (Fig. 1d). The polymerization step makes the micelles robust, stable for months and insensitive to dilution below CMC (0.11–0.12 mg mL<sup>-1</sup>). To meet physiological conditions, the pH was finally adjusted to 7.5 and osmolality to *ca.* 290 mOsm by addition of NaCl.

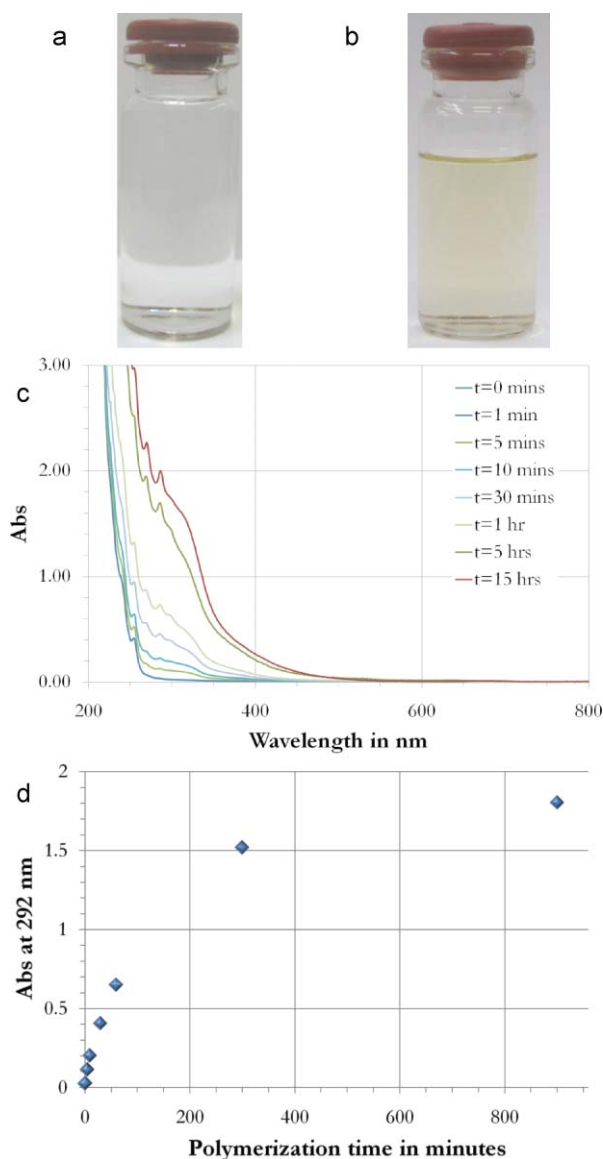


**Fig. 1** Pictures of (a) unpolymersed and (b) polymersed micelle solutions. Evolution of absorbance as a function of polymerization time of amphiphile **1** (c), (d).

The structure of the polymerized micelles was characterized by transmission electron microscopy (TEM) and dynamic light scattering (DLS). Both TEM observation of negatively stained

samples (Fig. 2a) and DLS data (Fig. 2b) showed spherical structures with an average diameter of *ca.* 6 nm (2–9 nm size distributions as determined by DLS), compared to that of non-polymerized micelles of 7 nm.

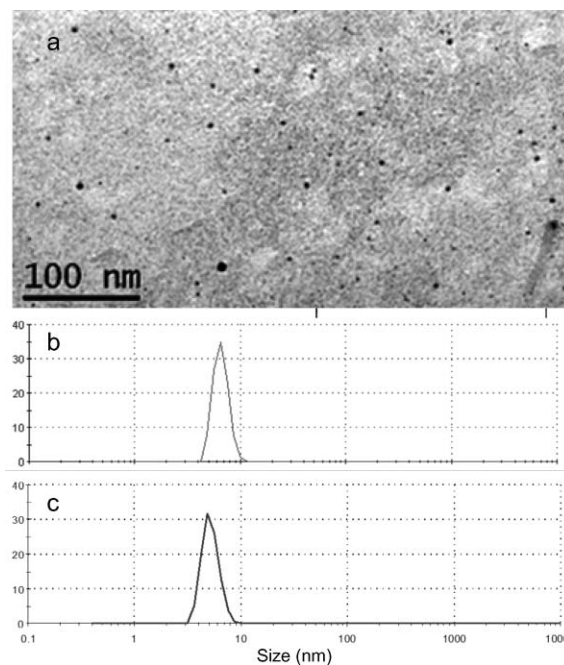


**Fig. 2** (a) TEM picture of polymerized micelles. Size distribution in number (%) of non-polymerized (b) and polymerized (c) micelles solutions.

The polymerized micelles were then used as a solubility enhancer of hydrophobic therapeutic molecules (TM) toward potential drug delivery applications. Molecules involved in this study are: an *E*-ring keto analogue of camptothecin (CPTD), a flavone derivative (FLD), and paclitaxel (Fig. 3). They all intrinsically exhibit very low solubility in water ( $\leq 2 \mu\text{g mL}^{-1}$ , Table 1).

Experiments showed a general increase of the solubility of the different therapeutic molecules (TM) by a factor ranging from

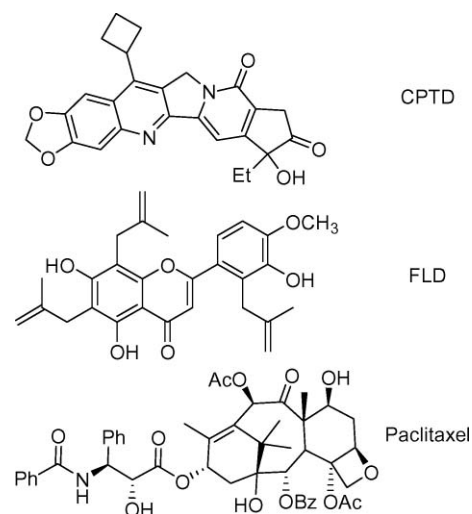


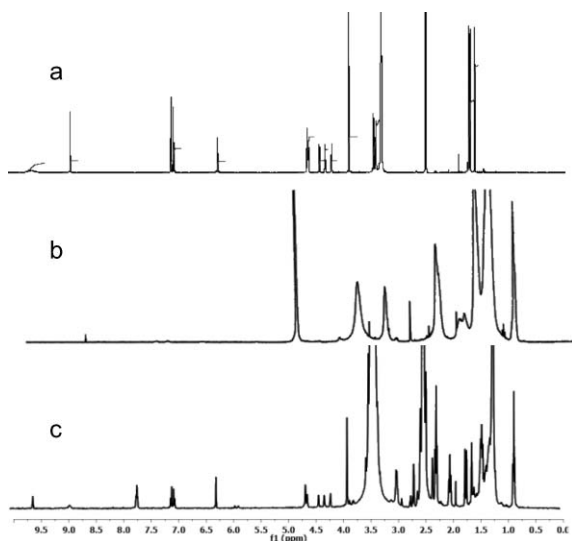
**Fig. 3** Chemical structures of *E*-ring keto analogue of camptothecin (CPTD), flavone derivative (FLD), and paclitaxel.

**Table 1** Solubilization of therapeutic molecules by polymerized micelles

TM	TM solubility in water/ $\mu\text{g cm}^{-3}$	TM solubility in micelle soln/ $\mu\text{g cm}^{-3}$	Drug loading (mass balance, %)
CPTD	0.09	$9.00 \times 10^3$	47
FLD	0.20	$3.15 \times 10^3$	24
Paclitaxel	0.40	$4.55 \times 10^3$	31

11 000 to 100 000 and drug loading from 24% to 47%, which correspond to a drug intake of 3.15 mg (FLD) to 9 mg (CPTD) per 10 mg of micelles. It is to be noted that, in the case of paclitaxel, values of 11 000 and 31% were obtained for solubility enhancement and loading capacity, respectively. These values are comparable to those of other analogous nanometric carriers described in the literature<sup>21–24</sup> and designate our polydiacetylenic micelles as efficient cargo for the encapsulation of hydrophobic drugs.

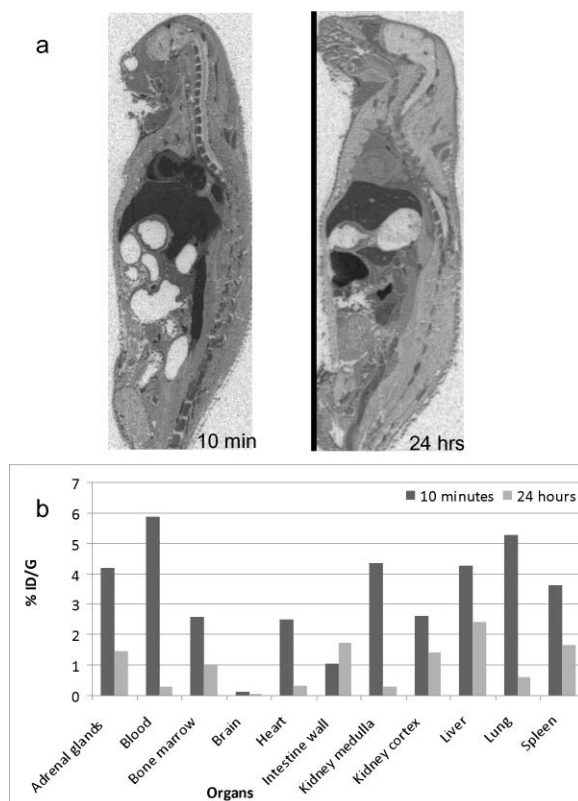
In the mean time,  $^1\text{H}$  NMR spectroscopy was used to study the drug/micelle complex. To this end, the overall sequence (preparation of the micelles and loading of the TM) was repeated in  $\text{D}_2\text{O}/\text{NaOD}$  and the samples were analyzed by  $^1\text{H}$  NMR. For example, the  $^1\text{H}$  NMR spectrum of the FLD/micelle complex exhibited intense broad aliphatic peaks corresponding to the micelle and weak broad aromatic signals that were attributed to FLD (Fig. 4b). The drug signals are masked by the micelle since the encapsulated molecules relax at the same rate as the surrounding polymer. To visualize both the load (FLD) and the container (micelle), the solution was freeze-dried and taken back in a dissociating solvent ( $\text{DMSO-d}_6$ ). The  $^1\text{H}$  NMR spectrum showed, this time, well-resolved and sharp peaks of FLD. This underlines the strong interaction between FLD and the micelle when in aqueous medium (Fig. 4c).

**Fig. 4**  $^1\text{H}$  NMR spectra of (a) FLD in  $\text{DMSO-d}_6$ , (b) FLD/micelle complex in  $\text{D}_2\text{O}$  and (c) FLD/micelle complex in  $\text{DMSO-d}_6$ .

To determine the effect of the polymerization step on drug loading capacity, we carried out comparative measurements of the inclusion of CPTD, in polymerized and non-polymerized micelles. While mass balance measurements indicated a drug loading of 47% for the polymerized formulation, a value of 3.3% was found for the

non-irradiated micelle. The non-irradiated micelle formed mainly a microsuspension of the TM that is filtered off after the inclusion process. This demonstrates that polymerization of the micelle is crucial for the loading and withholding of the drugs.

Preliminary studies were then undertaken to evaluate the pharmacokinetics of the polymeric micelles, more particularly their toxicity, biodistribution, and elimination. Acute toxicity was assessed in a single dose administration study to Wistar rats after bolus injection of the polymeric micelles in the caudal vein. No adverse event was observed over a three-day period at doses below  $100 \text{ mg kg}^{-1}$ . For distribution/elimination studies of the polymerized micelles, a  $^{14}\text{C}$ -labeled amphiphile **1** (compound **10**, see ESI†) was synthesized<sup>25,26</sup> and assembled into polydiacetylenic micelles. The latter (incorporating no drug) were administered to two male Wistar rats by bolus injection in the caudal vein at a dose of  $100 \text{ mg kg}^{-1}$  corresponding to  $4 \text{ MBq kg}^{-1}$  of radioactive material. The whole body tissue distribution of radioactivity was performed by radioluminography from sagittal sections ( $20 \mu\text{m}$  thick) at 10 min and 24 h after dosing (Fig. 5a). The radioluminograms showed wide and rapid distribution of the micelles in major tissues, but not in the brain (Fig. 5b). Slow renal elimination of the micelle was observed as only ca. 5% of the administered dose was detected in the urine, after 24 h. In addition, biliary excretion and faecal elimination seems to be operative since radioactivity was also detected in the faeces at 24 h.

**Fig. 5** (a) Radioluminograms and (b) tissue distribution (% dose/g) of total radioactivity at different time in Wistar rats after single intravenous administration of  $4 \text{ MBq kg}^{-1}$  of  $^{14}\text{C}$ -polymerized micelles.

The influence of the micelle on the pharmacokinetics of a therapeutic molecule was then investigated. Two different formulations



were prepared: (i) formulation A consisting of a nanosuspension of the free  $^{14}\text{C}$ -CPTD (reference formulation), and (ii) formulation B which was obtained by loading  $^{14}\text{C}$ -CPTD in non-labeled polymerized micelles. While formulation A is a stable suspension, B is a homogeneous solution. Each formulation was injected bolus *via* the caudal vein to a series of five C57 black male mice at a dose corresponding to  $5\text{ mg kg}^{-1}$  of CPTD ( $4\text{ MBq kg}^{-1}$ ). The mice were sacrificed at variable times, from 5 min to 48 h, and sagittal cuts were analyzed by radioluminography (Fig. 6a).

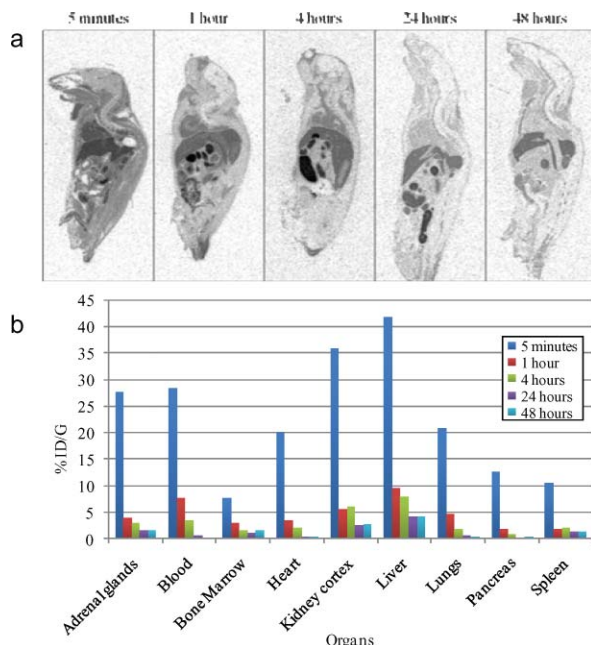


**Fig. 6** (a) Radioluminograms and (b) tissue distribution (% dose/g) of total radioactivity at different times in the C57 black male mice after single intravenous administration of  $4\text{ MBq kg}^{-1}$  of  $^{14}\text{C}$ -CPTD in polydiacetylenic micelles.

Five minutes after administration of formulation A, accumulation of CPTD in the liver, spleen, kidney cortex and lachrymal glands was observed, leaving only residual amounts of radioactivity in the blood compartment. In addition, the overall radioactivity decreased rapidly in the body to be virtually nil at 24 h.

It appears as striking evidence that the residence time of  $^{14}\text{C}$ -CPTD in the body is significantly improved when associated to the polymerized micelle as, this time, the radioactivity decreased slowly and steadily over a period of time greater than 48 h after dosing of the formulation B. The TM is mainly distributed to the liver, kidney cortex and, in a lesser proportion, to adrenal glands and spleen (Fig. 6b). Distribution and tissue elimination half-life increased compared to reference formulation A. Micelle encapsulation significantly slowed down migration of the drug from blood to tissues and decreased the elimination rate from the body.

It must be pointed out that, with both formulations, a large quantity of radioactivity was observed at some point in the intestine, evidence that biliary excretion is a major elimination pathway for CPTD and/or its metabolites.

## Conclusions

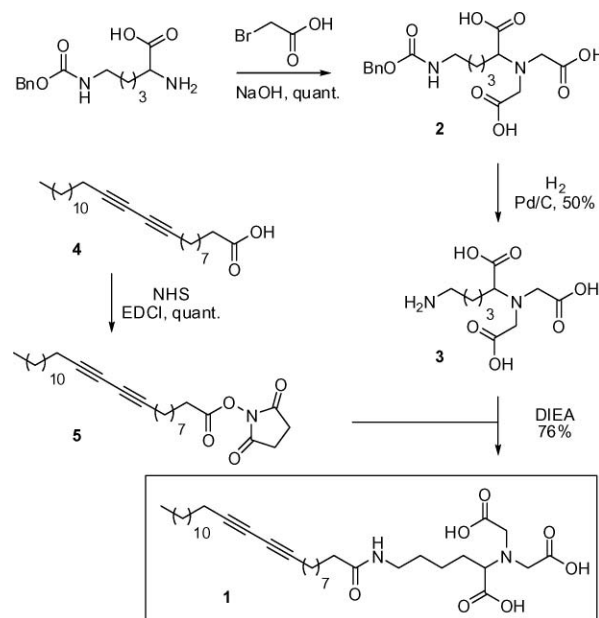
In conclusion, we report here a new drug carrier system based on the self-assembly and polymerization of specifically designed amphiphiles. The polydiacetylenic micelles provide effective hydrophobic drugs loading and solubility enhancement. The distribution/clearance studies are promising as the body residence time of drugs is increased. No specific organ seems to be targeted and the primary pathway of excretion of both the drug and the micelles is biliary.

## Experimental procedures

### Materials and methods

Chemicals were purchased from Aldrich. Common organic solvents were used without further purification.  $\text{CH}_2\text{Cl}_2$  was distilled over  $\text{CaH}_2$  prior to use. NMR spectra were recorded on a Bruker Advanced 400 at 400 MHz ( $^1\text{H}$ ) and 100 MHz ( $^{13}\text{C}$ ). Chemical shifts are given in ppm relative to the NMR solvent residual peak. Mass spectra were recorded using a MarinerTM ESI-TOF spectrometer. IR-spectra were recorded using a Perkin-Elmer 2000 FT-IR. Wavenumbers are given in  $\text{cm}^{-1}$  at their maximum intensity. Size distribution of micelles was measured using a Zetasizer Nano series (Malvern).

### Synthesis of amphiphile 1 (Scheme 2)



**Scheme 2** Synthesis of photo-polymerizable amphiphile 1.

***N*<sup>6</sup>-Carboxybenzyloxy-*N*<sup>2</sup>,*N*<sup>2</sup>-bis(carboxymethyl)lysine (2).** Bromoacetic acid (10.82 g, 4 equiv.) was solubilized in 120 mL of 1 N NaOH. The solution was cooled to 0 °C and *Z*-lysine (5.39 g, 19 mmol, 1 equiv.) in 30 mL of 1 N NaOH was added dropwise. The solution was stirred at r.t. for 2 h and at 50 °C for 12 h. The solution was cooled to 0 °C and acidified with 37% HCl. The white precipitate was collected by filtration and dried under vacuum over  $\text{P}_2\text{O}_5$ . Yield: quant.  $^1\text{H}$  NMR ( $\text{DMSO}-d_6$ ):

7.25–7.40 (m, 5H), 7.21 (t, 1H,  $J = 5.5$  Hz), 4.98 (s, 2H), 3.46 (m, 4H), 3.33 (t, 1H,  $J = 7.2$  Hz), 2.85–3.05 (m, 2H), 1.15–1.65 (m, 6H).  $^{13}\text{C}$  NMR (DMSO- $d_6$ ): 174.5, 174.0 (2C), 156.5, 137.6, 128.7 (2C), 128.0 (3C), 65.4, 64.9, 59.8, 54.2, 29.5–29.6 (2C); 23.4. MS (ESI $^+$ /TOF)  $m/z$ : 397 [M + H] $^+$ . IR (KBr,  $\text{cm}^{-1}$ ): 3364, 3042, 2935, 1721, 1523, 1278, 1131, 1013, 905, 742, 683.

**$N^2$ -Bis(carboxymethyl)lysine (3).**  $N^6$ -Carboxybenzyloxy- $N^2,N^2$ -bis(carboxymethyl)lysine **2** (7.6 g, 19.2 mmol, 1 equiv.) was solubilized in 200 mL of MeOH. 300 mg of 10% Pd/C was added and the flask was purged 4 times with  $\text{N}_2$ , and 4 times with  $\text{H}_2$ . The solution was stirred under  $\text{H}_2$  at r.t. for 12 h. The precipitate was collected by filtration and taken back into  $\text{H}_2\text{O}$ . Palladium was filtered off, and the solution freeze dried. Yield: 50%.  $^1\text{H}$  NMR (DMSO- $d_6$ ): 3.75–3.9 (m, 5H), 2.89 (t, 2H,  $J = 7.2$  Hz), 1.4–1.9 (m, 6H).  $^{13}\text{C}$  NMR (DMSO- $d_6$ ): 171.9 (1C), 170.1 (2C), 67.6 (1C), 55.1 (2C), 38.9 (1C), 26.3 (2C), 22.9 (1C). MS (ESI $^+$ /TOF)  $m/z$ : 263 [M + H] $^+$ , 285 [M + Na] $^+$ . IR (KBr,  $\text{cm}^{-1}$ ): 3498, 3324, 2996, 2975, 1750, 1634, 1401, 1263, 1159, 984, 876, 751.

**2,5-Dioxo-pyrrolidin-1-yl pentacosa-10,12-diynoate (5).** Pentacosa-10,12-diynoic acid **4** (1 g, 2.7 mmol, 1 equiv.),  $N$ -(3-dimethylaminopropyl)- $N'$ -ethylcarbodiimide (0.78 g, 1.5 equiv.) and  $N$ -hydroxysuccinimide (0.5 g, 1.8 equiv.) were solubilized in 50 mL of anhydrous  $\text{CH}_2\text{Cl}_2$ . The solution was stirred at r.t. for 12 h under  $\text{N}_2$  and quenched with  $\text{H}_2\text{O}$ . The aqueous phase was extracted twice with  $\text{CH}_2\text{Cl}_2$ . The organic phases were collected, dried and concentrated under vacuum to give **5** as a white solid. Yield: quant.  $^1\text{H}$  NMR (DMSO- $d_6$ ): 2.7–2.9 (m, 4H), 2.58 (t, 2H,  $J = 7.2$  Hz), 2.22 (t, 4H,  $J = 7.2$  Hz), 1.72 (q, 2H,  $J = 7.2$  Hz), 1.49 (t, 2H,  $J = 7.2$  Hz), 1.2–1.42 (m, 28H), 0.86 (t, 3H,  $J = 7.2$  Hz).  $^{13}\text{C}$  NMR (DMSO- $d_6$ ): 169.2 (2C), 168.5 (1C), 77.6 (1C), 77.3 (1C), 65.3 (1C), 65.2 (1C), 31.8 (1C), 28.1–30.7 (16C), 24.4 (1C), 22.5 (1C), 18.9 (2C), 13.9 (1C). MS (ESI $^+$ /TOF)  $m/z$ : 472 [M + H] $^+$ , 494 [M + Na] $^+$ .

**$N^6$ -Pentacosa-10,12-diynoyl- $N^2,N^2$ -bis(carboxymethyl)lysine (1).**  $N^2,N^2$ -Bis(carboxymethyl)lysine **3** (1 g, 1.2 equiv.) and 3.1 mL of  $\text{NEt}_3$  (7 equiv.) were dispersed in 100 mL of DMF.  $\text{H}_2\text{O}$  was added dropwise until complete solubilization. 2,5-dioxo-pyrrolidin-1-yl pentacosa-10,12-diynoate **5** (1.44 g, 3.05 mmol, 1 equiv.) in 50 mL of DMF was then added. The solution was stirred at r.t. for 12 h. The solution was concentrated under vacuum, taken into  $\text{H}_2\text{O}$ , and acidified with 37% HCl. The white solid was filtered off, washed with water and dried overnight under vacuum and  $\text{P}_2\text{O}_5$ . Yield: 76%.  $^1\text{H}$  NMR (DMSO- $d_6$ ): 7.68 (t, 1H,  $J = 5.6$  Hz), 3.39–3.50 (AB, 4H,  $J_{\text{AB}} = 17.6$  Hz), 3.35 (t,  $J = 7.3$  Hz, 1H), 2.97 (m, 2H), 2.24 (t, 4H,  $J = 6.8$  Hz), 2.00 (t, 2H,  $J = 7.2$  Hz), 1.1–1.6 (m, 38H), 0.82 (t, 3H,  $J = 6.8$  Hz).  $^{13}\text{C}$  NMR (DMSO- $d_6$ ): 174.3 (1C), 173.6 (2C), 172.2 (1C), 78.0 (2C), 65.7 (1C), 64.7 (2C), 53.7 (2C), 38.6 (1C), 35.8 (1C), 28.0–31.7 (16C), 25.7 (1C), 23.5 (1C), 22.5 (1C), 18.7 (2C), 14.3 (1C). MS (ESI/TOF)  $m/z$ : (ESI $^+$ ) 619 [M + H] $^+$ , 641 [M + Na] $^+$ , (ESI $^-$ ) 617 [M – H] $^-$ . ESI HRMS [M – H] $^-$  calcd for  $\text{C}_{35}\text{H}_{57}\text{N}_2\text{O}_7$ : 617.4166; found: 617.4165. IR (KBr,  $\text{cm}^{-1}$ ): 3323, 2925, 2853, 1929, 1732, 1645, 1546, 1464, 1425, 1256, 983, 892, 720.

### Synthesis of polymerized micelles

A solution of the diacetylenic amphiphile **1** (10 mg  $\text{mL}^{-1}$  in 0.01M NaOH—pH = 12) was sonicated with an ultrasonic probe to

produce monodisperse micelles. The solution was polymerized by irradiation at 254 nm for 5 h (low pressure mercury UV lamp—Heraeus). The pH was finally adjusted to 7.5 and osmolality to ca. 290 mOsm by addition of NaCl.

### Drug loading of hydrophobic therapeutic molecules (TM)

In a standard experiment, 40 mg of the drug was dispersed and stirred for 12 h at 50 °C in 2 mL of an aqueous solution of the micelles (10 mg  $\text{mL}^{-1}$ ). The solution was then filtered (0.2  $\mu\text{m}$ ) to remove unsolubilized drug and to yield a clear solution with no particles in suspension. The solution was freeze-dried and weighed. In parallel, the same sequence was repeated, but with no drug. The weight of solubilized therapeutic molecules can then be determined by mass balance of the two experiments. From this value, a drug loading was calculated by dividing the mass of the drug by the mass of the micelles incorporating the drug (see ESI $^\dagger$ ).

### Distribution/elimination study of $^{14}\text{C}$ -polymerized micelles

All experiments were performed in accordance with European regulations on care and use of laboratory animals. Polymerized micelles were administered by bolus injection in the caudal vein at 100 mg  $\text{kg}^{-1}$  (4 MBq  $\text{kg}^{-1}$ ) to two male Wistar rats. Rats were sacrificed at 10 min and 24 h after administration for quantitative tissue distribution of radioactivity.

### Distribution study of $^{14}\text{C}$ -CPTD

Each  $^{14}\text{C}$ -CPTD formulation was injected at a dose of 5 mg  $\text{kg}^{-1}$  and 4 MBq  $\text{kg}^{-1}$  by bolus injection in the caudal vein to a series of five C57 black male mice. Mice were sacrificed at variable times (5 min to 48 h) after administration for quantitative tissue distribution of radioactivity.

### Quantitative tissue distribution of radioactivity

Frozen rats and mice were individually embedded in carboxymethylcellulose which was subsequently frozen. Using a cryomicrotome (PMV 450 – LKB), 20  $\mu\text{m}$  sagittal sections were cut from each animal to reveal the tissues of interest. The quantification of the freeze dried sagittal sections was obtained by radioluminography (BAS 2000, FUJI PHOTO FILM Co. Ltd.), using standard calibration sources prepared by mixing radioactive compound with blood samples.

### Acknowledgements

We thank A. Petit, N. Bongibault-Besnard and N. Masson-Lancelot for NMR studies.

### References

- 1 K. Letchford and H. Burt, *Eur. J. Pharm. Biopharm.*, 2007, **65**, 259.
- 2 T. M. Allen and P. R. Cullis, *Science*, 2004, **303**, 1818.
- 3 M. J. McKeage, S. J. Berners-Price, P. Galettis, R. J. Bowen, W. Brouwer, L. Ding, L. Zhuang and B. C. Baguley, *Cancer Chemother. Pharmacol.*, 2000, **46**, 343.
- 4 T. W. Moody, S. A. Mantey, T. K. Pradhan, M. Schumann, T. Nakagawa, A. Martinez, J. Fuselier, D. H. Coy and R. T. Jensen, *J. Biol. Chem.*, 2004, **279**, 23580.
- 5 J. Liu, P. Zahedi, F. Zeng and C. Allen, *J. Pharm. Sci.*, 2008, **97**, 3274.

- 6 Q. Li, Y. Zu, R. Shi, L. Yao, Y. Fu, Z. Yang and L. Li, *Bioorg. Med. Chem.*, 2006, **14**, 7175.
- 7 W.-S. Fang and X.-T. Liang, *Mini. Rev. Med. Chem.*, 2005, **5**, 1.
- 8 M. Skwarczynski, Y. Hayashi and Y. Kiso, *J. Med. Chem.*, 2006, **49**, 7253.
- 9 J. Ogier, T. Arnauld and E. Doris, *Future Med. Chem.*, 2009, **1**, 693.
- 10 H. Hillaireau, P. Couvreur, in *Polymers in drug delivery*, CRC Press LLC, Boca Raton, 2006, pp. 101–110.
- 11 N. Nishiyama and K. Kataoka, *Pharmacol. Ther.*, 2006, **112**, 630.
- 12 V. P. Torchilin, *Nat. Rev. Drug Discovery*, 2005, **4**, 145.
- 13 C. L. Lee, J. A. MacKay, J. M. Fréchet and F. C. Szoka, *Nat. Biotechnol.*, 2005, **23**, 1517.
- 14 N. Mackiewicz, G. Surendran, H. Remita, B. Keita, G. Zhang, L. Nadjo, A. Hagge, E. Doris and C. Mioskowski, *J. Am. Chem. Soc.*, 2008, **130**, 8110.
- 15 T. Shimizu, M. Masuda and H. Minamikawa, *Chem. Rev.*, 2005, **105**, 1401.
- 16 C. Kollmar, *J. Chem. Phys.*, 1993, **98**, 7210.
- 17 C. Itoh, T. Kondoh and K. Tanimura, *J. Phys. Soc. Jpn.*, 1999, **68**, 1711.
- 18 Y. Okawa and M. Aono, *J. Chem. Phys.*, 2001, **115**, 2317.
- 19 H. Sixl, *Adv. Polym. Sci.*, 1984, **63**, 49.
- 20 H. Sixl, C. Kollmar, R. Huber and E. Sigmund, *Phys. Rev. B: Condens. Matter*, 1987, **36**, 2747.
- 21 S. C. Lee, K. M. Huh, J. Lee, Y. C. Cho, R. E. Galinsky and K. Park, *Biomacromolecules*, 2007, **8**, 202.
- 22 S. Li, B. Byrne, J. Welsh and A. F. Palmer, *Biotechnol. Prog.*, 2007, **23**, 278.
- 23 R. E. Richard, M. Schwarz, S. Ranade, A. K. Chan, K. Matyjaszewski and B. Sumerlin, *Biomacromolecules*, 2005, **6**, 3410.
- 24 X. Shuai, T. Merdan, A. K. Schaper, F. Xi and T. Kissel, *Bioconjugate Chem.*, 2004, **15**, 441.
- 25 D. H. R. Barton, D. Crich and W. B. Motherwell, *J. Chem. Soc., Chem. Commun.*, 1993, 939.
- 26 O. Loreau, A. Maret, D. Poullain, J. M. Chardigny, J. L. Sébédio, B. Beaufrère and J. P. Noel, *Chem. Phys. Lipids*, 2000, **106**, 65.